

# Kinematic Modelling of Humanoid Robot Based on Vectorial Approach

Nacer Hadidi, Chawki Mahfoudi, Mohamed Bouaziz, Zaharuddin Mohamed, and Ahcene Bouzida

**Abstract**— The present work is dedicated to the study of the inverse kinematics solution of a humanoid bipedal robot with 30 degrees of freedom using a newly approach based on vectors that generated from the geometric space of the robot. The solutions of the inverse kinematics problem for all joints articulations are carried out through a simple and linear equations. Finally, simulations of results are performed through harmonization of trajectories of end effectors of the robot's members.

**Keywords**— biped robot, Humanoid robot, inverse kinematics, robotic, vectors calculus.

## NOMENCLATURE

DKM: Direct Kinematic Model.  
 IKM : Inverse Kinematic Model.  
 SSP : Simple support phase.  
 DSP : Double Support Phase.  
 $C(\theta_i) : \cos(\theta_i)$   
 $S(\theta_i) : \sin(\theta_i)$

## I. INTRODUCTION

Robotics has captivated a portion of the scientific community due to its alluring prospects across various domains [1]. Indeed, robotics has progressed rapidly, transcending what was once considered science fiction into reality. Among the many branches of robotics, humanoid bipedal robots have garnered intense research in recent years [2-4]. Researchers continue to tackle challenges in various aspects, striving for advancements beyond completed studies. Researchers have emphasized various concepts within this domain, including mechanical design, kinematic and dynamic modeling...etc. Mechanical design aims to create human-sized robots with a high degree of freedom within a compact volume, presenting a significant challenge [5], [6]. Consequentially, mathematical modeling in robotics makes another side of channelling, like kinematic modeling. In fact, this last one (kinematic modeling) plays a crucial role in

providing the foundational equations used in robot's dynamics and control.

This paper presents an inverse kinematics study of a bipedal robot with a significant number of degrees of freedom (30 DOF). The robot is divided on six main parts, each parts is modeled in its proper frame. However, this last one is reconducted in the principal frame on the robot's hip which will be expressed on the global frame. Basically, according to the used approach, each angle that represent one degrees of freedom is described by three vectors from which should be expressed by its magnitude and its rotation sense.

## II. THE MODEL OF THE BIPED ROBOT

The robot model has 30 degrees of freedom (30 DOF) which allow great mobility (Fig. 1).

The robot structure is divided into 06 main parts: the trunk, the neck-head, the upper limbs (right and left arms), and the lower limbs (right and left legs). A primary reference frame is fixed at the hip. Than, all frames within the robot structure are defined according to the Denavit-Hartenberg (DH) convention as it is illustrated in Fig. 1. This allows providing the different matrices that will be used in the Forward Kinematics (Fk). Table 1 summarizes the lengths of the various links of the robot.

Manuscript received May 22, 2024; revised July 4, 2024.

N. Hadidi is with dept. of mechanical Engineering, Ecole Nationale Supérieure des sciences appliquées, Algiers, ALGERIA. (email: nacer.hadidi@ensta.edu.dz).

C. Mahfoudi is with dept. of Mechanical Engineering, Univ. of Larbi Ben M'hidi, Oum El Bouaghi, ALGERIA. (email: c\_mahfoudi\_dz@yahoo.fr).

M. Bouaziz is with dept. of mechanical Engineering, Ecole Nationale Polytechnique, Algiers, ALGERIA. (email: mbouaziz@yahoo.fr).

Z. Mohamed is with dept. Mechatronics, Faculty of Electrical Engineering, Universiti Teknologi Malaysia, Johor Bahru, MALAYSIA. (email: zahar@utm.my).

A. BOUZIDA is with dept. Elctrical Engineering, Univ. Akli Mohand Oulhadj, Bouira, ALGERIA. (email: a.bouzida@univ-bouira.dz).

Digital Object Identifier (DOI): 10.53907/enpesj.v4i1.271

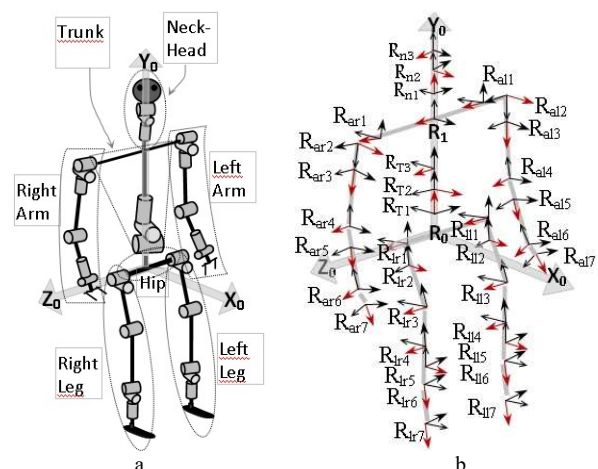


Fig.1: Robot Model. a. Kinematic diagram of the robot. b. Different frames of the robot.

**Table 1.**  
LENGTHS OF ROBOT LINKS

MECHANISMS	ELEMENTS	LENGTHS (m)
Upper limb	Fore-arm	$L_{fo} = 0.28$
	arm	$L_a = 0.30$
	hand	$L_h = 0.10$
Lower limb	Leg	$L_l = 0.30$
	Shin	$L_s = 0.30$
	feet	$L_f = 0.10$
	Middle part	Trunc
	Hip	$L_H = 0.10$
Head-neck	Head-neck	$L_n = 0.10$

### III. KINEMATIC MODELING OF THE ROBOT

Kinematic modeling serves as the foundation in robotics, known through the Forward Kinematic Model (FKM) and Inverse Kinematic Model (IKM).

#### A. Forward kinematic Model

According to DH convention, the transformation from basic frame to end-effector is expressed by the following matrix given in (1).

$$\begin{bmatrix} s_x n_x a_x P_{dx} \\ s_y n_y a_y P_{dy} \\ s_z n_z a_z P_{dz} \\ 0 & 0 & 0 & 1 \end{bmatrix} = {}^0T_1 {}^1T_2 {}^2T_3 \dots {}^{n-1}T_n \quad (1)$$

$$= [\mathbf{S} \mathbf{N} \mathbf{A} \mathbf{P}]$$

Where:

$[\mathbf{S} \mathbf{N} \mathbf{A} \mathbf{P}]$ : exprime orientation and position of end-effector in basic frame.  ${}^{i-1}T_i$  is a matrix of homogeneous transformation between two successive frames ( $i = 1 \dots n$ ).

#### B. Principle of the Inverse Kinematic Calculation Approach.

In this section, we use the new proposed approach that established by [7] which is foned on a vectorial description of the robot to solve the IK problem. One of the most useful mathematical formula that used to be explored in robotics in providing analythecal solution of variable articulation  $\beta$  (angle) expressed between two vectors,  $\vec{U}$  and  $\vec{V}$ , is given in (2).

$$\beta = \text{atan2}(\sin(\vec{U}, \vec{V}), \cos(\vec{U}, \vec{V})) \quad (2)$$

Subsequently, the formula in (2) has an advantage in providing the correct orientation and value of the angle  $\beta$  at any quadrant of the cercle. In addition, a suitable relation between  $\sin(\vec{U}, \vec{V})$  and  $\det(\vec{n}_U, \vec{n}_V, \vec{n}_W)$  is established by [7].

$$\sin(\vec{U}, \vec{V}) = \det(\vec{n}_U, \vec{n}_V, \vec{n}_W) \quad (3)$$

Where:

$\vec{n}_U = \frac{\vec{U}}{U}$ ,  $\vec{n}_V = \frac{\vec{V}}{V}$  and  $\vec{n}_W = \frac{\vec{W}}{W}$  are, respectively, unit vectors of  $\vec{U}$ ,  $\vec{V}$  and  $\vec{W}$ . The vector  $\vec{W}$  could be the cross product of  $\vec{U}$  and  $\vec{V}$  or any other orthogonal vector to the plane formed by  $\vec{U}$  and  $\vec{V}$  (UV-plane).

A notable characteristic of determinant regarding its sign emerges when two columns are swapped [8].

$$\det(\vec{n}_U, \vec{n}_V, \vec{n}_W) = (-1)\det(\vec{n}_V, \vec{n}_U, \vec{n}_W)$$

By knowing, the determinant calculated from the vectors concerning the angle and its cosine value, equation (2) fully determines the angle, including both its sign and value. Hence, equation (2) can be written as shown in (3)

$$\beta = \text{atan2}(\det(\vec{n}_U, \vec{n}_V, \vec{n}_W), \cos(\vec{U}, \vec{V})) \quad (3)$$

#### C. Calculation and identification of angles of the bipedal robot.

As mentioned in the introduction, the biped robot is divided into 06 parts. Therefore, we proceed to model each one separately.

##### 1) Inverse Kinematic Modeling of the Trunk

The movement of the trunk is generated by three joint angles (Fig.2).

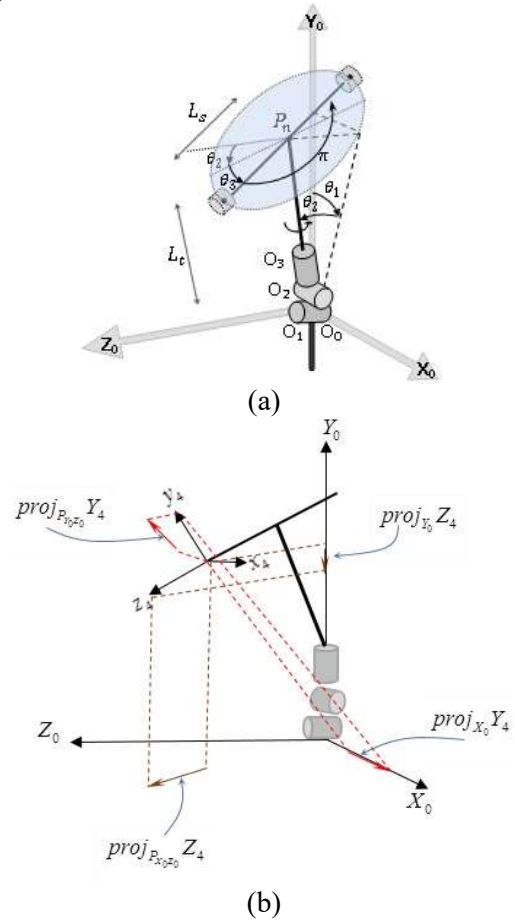


**Fig.2:** Geometric Description of the Trunk and Shoulder mechanism. a. Geometric Modeling of the Trunk. b. Current Position of the Shoulder.

The joint angle  $\theta_3$  is determined by the following three vectors:  $\text{proj}_{P_{X_0Z_0}} \vec{Z}_4$ ,  $\vec{Z}_0$  et  $\vec{Y}_0$ .

Knowing that:  $\text{proj}_{P_{X_0Z_0}} \vec{Z}_4 = \vec{Z}_4 - \text{proj}_{Y_0} \vec{Z}_4$ . is the projection of the vector  $\vec{Z}_4$  onto the plane  $P_{X_0Z_0}$ .

$\vec{Z}_4$  is a direction cosine vector of the desired shoulder position matrix.

So,  $\theta_3$  is expressed by (4):

$$\theta_3 = \text{atan2}(\det_{\theta_3}, \cos \theta_3) \quad (4)$$

Where:  $\det_{\theta_3} = \det[\vec{Z}_0 \text{ proj}_{P_{X_0Z_0}} \vec{Z}_4 \vec{Y}_0]^T$  and  $\cos \theta_3 = \vec{Z}_0 \cdot \text{proj}_{P_{X_0Z_0}} \vec{Z}_4$

Determining the joint angles  $\theta_1$  and  $\theta_2$  involves first determining the position of the midpoint ( $P_n$ ) through the matrix giving the desired shoulder position via the following relationship :

$$\overrightarrow{OP_n} = \overrightarrow{OP_s} - L_s \overrightarrow{A_4}$$

Where

$\overrightarrow{OP_n}$ : Vector expressing midpoint of shoulders.

$\overrightarrow{OP_s}$ : Vector expressing shoulder position.

$L_s$ : Length of shoulder.

$\overrightarrow{A_4}$ : Vector of cosine direction of shoulder's frame on z-axis.

The angle  $\theta_1$  is determined by the following vectors:

$$proj_{P_{X_0Y_0}} \overrightarrow{n_{P_n}}, \overrightarrow{Y_0} \text{ and } \overrightarrow{Z_0}.$$

Given that:  $proj_{P_{X_0Y_0}} \overrightarrow{n_{P_n}} = \overrightarrow{n_{P_n}} - proj_{Z_0} \overrightarrow{n_{P_n}}$  it is the projection of the vector  $\overrightarrow{n_{P_n}}$  onto the plane  $P_{X_0Y_0}$

Where:  $\overrightarrow{n_{P_n}}$  is the unit vector of  $\overrightarrow{OP_n}$ .

$$\theta_1 = atan2(det_{\theta_1}, cos(\theta_1)) \quad (5)$$

With:  $det_{\theta_1} = det[\overrightarrow{Y_0} \ proj_{P_{X_0Y_0}} \overrightarrow{n_{P_n}} \ \overrightarrow{Z_0}]^T$  and  $cos(\theta_1) = \overrightarrow{Y_0} \cdot proj_{P_{X_0Y_0}} \overrightarrow{n_{P_n}}$

Angle  $\theta_2$  is determined by the following vectors:  $proj_{P_{Y_0Z_0}} \overrightarrow{n_{P_n}}, \overrightarrow{Y_0}$  et  $\overrightarrow{X_0}$

Given that:  $proj_{P_{Y_0Z_0}} \overrightarrow{n_{P_n}} = \overrightarrow{n_{P_n}} - (proj_{X_0} \overrightarrow{n_{P_n}})$ . It is the projection of the vector  $\overrightarrow{n_{P_n}}$  onto the plane  $P_{Y_0Z_0}$

$$\theta_2 = atan2(det_{\theta_2}, cos(\theta_2)) \quad (6)$$

With:  $det_{\theta_2} = det[\overrightarrow{Y_0} \ proj_{P_{Y_0Z_0}} \overrightarrow{n_{P_n}} \ \overrightarrow{X_0}]^T$  and  $cos(\theta_2) = \overrightarrow{Y_0} \cdot proj_{P_{Y_0Z_0}} \overrightarrow{n_{P_n}}$

### 2) Inverse Kinematic Modeling of the Neck-Head Mechanism

The movement of the head is governed by the joints incorporated at the robot's neck  $\theta_4, \theta_5$  and  $\theta_6$  as shown in Fig.3.

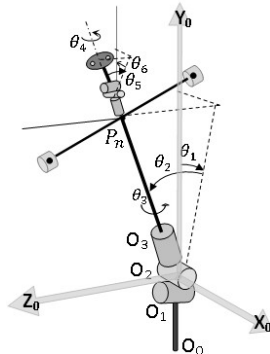


Fig.3: Joints angles of the Neck-Head.mechanism.

During the robot's movement, the head that is connected to trunk at midpoint by the neck with three joint articulations is assumed to be on the vertical straight position.

Therefore, and from Fig.3, the joints  $\theta_5$  and  $\theta_6$  must respectively have the same values as  $\theta_2$  and  $\theta_1$  of the trunk, but in opposite rotation, as expressed in (7). Also, the Joint  $\theta_4$  is assumed to be stationary.

$$\theta_5 = -\theta_2 \quad et \quad \theta_6 = -\theta_1 \quad (7)$$

### 3) Inverse Kinematic Modeling of the Upper Limb (Arm).

Fig. 4 depicts a right upper limb with 6 degrees of freedom of the bipedal robot distributed among three links: the upper arm ( $L_a$ ), the forearm ( $L_{fa}$ ), and the hand ( $L_h$ )

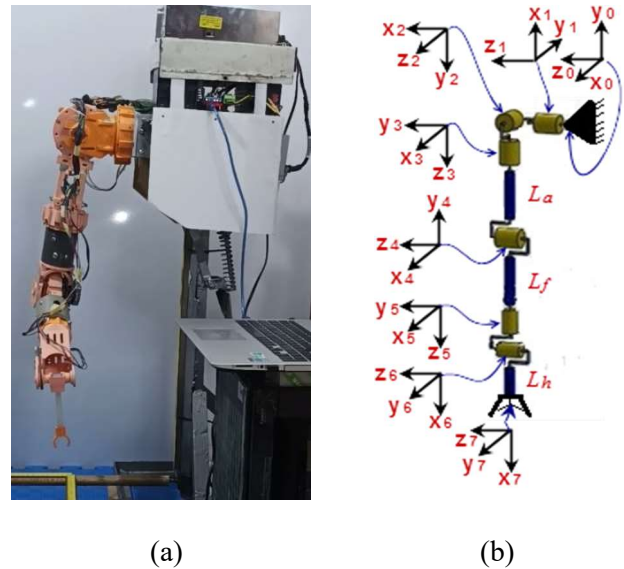


Fig.4: Right upper limb of a bipedal robot and assignment of frames according to the DH convention. a. Image of the robot arm. b. inematic chain of the robot arm [7].

In this work, the following assumptions are considered:

- The shoulder, with its 3 degrees of freedom (3DOF), has its rotation axes intersecting at the same point. Therefore, the rotational movement of the shoulder can be treated as a single geometric point.
- Similarly, the same assumption is applied to the wrist, which has 2 DOF.

Fig. 5 depicts a geometric parametrization of the robot (geometric entities) that will be used in the process of solving the IKM.

The strategy to solve the inverse geometric problem is divided into two phases:

- the first phase involves in determining the geometric entities that allowed the determination of the vectors defining each joint.
- The second phase focuses on determining the angles of each joint.

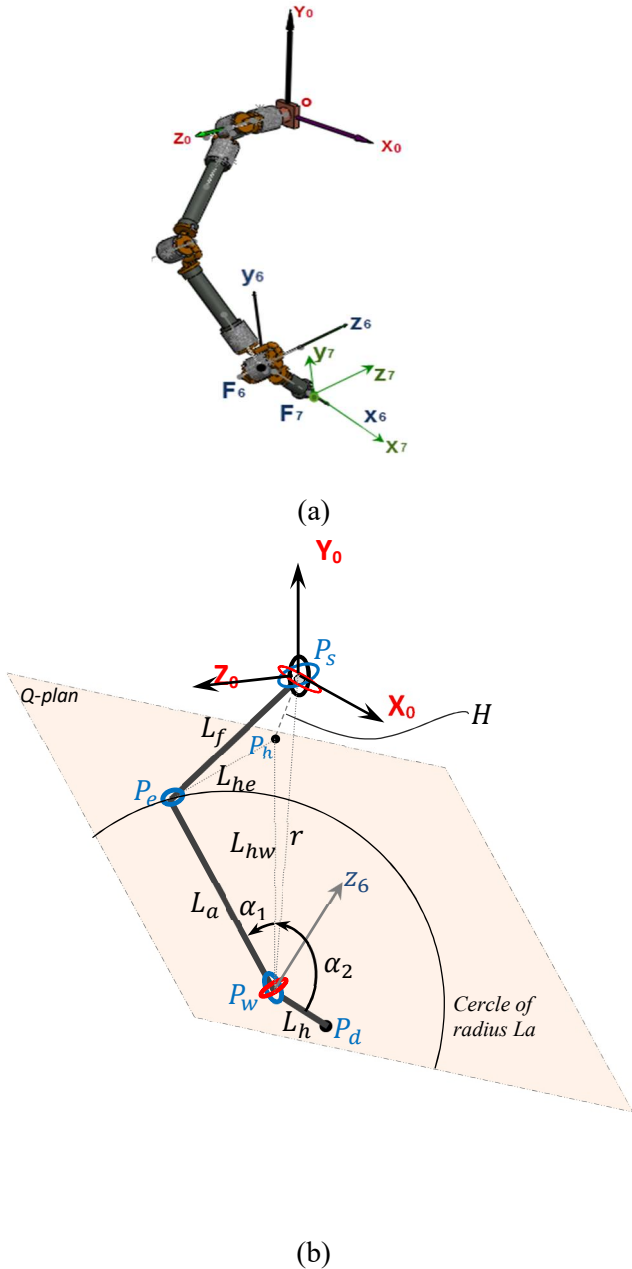


**Fig.5:** Geometric parametrization of a right upper limb of a bipedal robot. a. Robot configuration with assignment of main frames. b. Geometric entities [7].

#### a) Calculation of Geometric Entities of the Robot

To do this, the following strategy is adopted:

- Determine the position of the wrist.
- Determine the position of the elbow.

The position of the wrist is given by (8).

$$\overrightarrow{OP_w} = \overrightarrow{OP_d} - L_h \overrightarrow{S_6} \quad (8)$$

where:

$\overrightarrow{OP_w} = (P_{wx}, P_{wy}, P_{wz})^T$  and  $\overrightarrow{OP_d} = (P_{dx}, P_{dy}, P_{dz})^T$  respectively are the coordinates of the wrist position and the desired position of the end effector (hand).  $L_h$  is the length between wrist and hand. We define the circle of the center  $P_w$  (wrist position) and radius  $L_f$  (forearm length) on the plane  $Q$ -plan that is defined by

$$\overrightarrow{OP_c} = \overrightarrow{OP_w} + L_f \cos(\varphi) \overrightarrow{S_6} + L_f \sin(\varphi) \overrightarrow{N_6} \quad (9)$$

Where:

$\overrightarrow{OP_e} = (P_{ex}, P_{ey}, P_{ez})^T$  and  $\overrightarrow{OP_w} = (P_{wx}, P_{wy}, P_{wz})^T$  are, respectively, the coordinates of the circumference of the circle and the center of the circle.  $\overrightarrow{S_6}$  and  $\overrightarrow{N_6}$  are, respectively, the unit vectors of the  $x_6$ -axis et  $y_6$ -axis. And  $\varphi$  is the angle between  $x_6$ -axis and  $\overrightarrow{V_{we}}$  (vector defined by wrist and elbow). Thus, from (9), the position of the elbow is determined by the vector of coordinates given in (10).

$$\overrightarrow{OP_c} = \overrightarrow{V_{oe}} = (P_{ex}, P_{ey}, P_{ez})^T \quad (10)$$

By determining the necessary geometric entities, we proceed for identification of joint angles.

#### b) Calculation of Arm Joint Angles

Geometrically, three vectors (Fig.6), from which two mathematical arguments ( $\arg 1, \arg 2$ ) are expressed and will be used in (6), describe each joint angle.

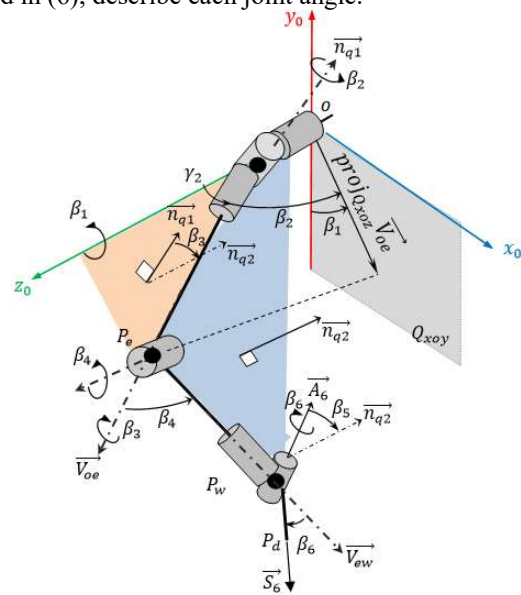


**Fig.6:** Vectorial description of arm's joint angles.

#### • Joint angle $\beta_1$

The vectors define the angle:

$\text{proj}_{Q_{xoz}} \overrightarrow{V_{oe}}, -\overrightarrow{y_0}$  and  $\overrightarrow{z_0}$ . Given that :

$$\det_{\beta_1} = \det(-\overrightarrow{y_0}, \text{proj}_{Q_{xoz}} \overrightarrow{V_{oe}}, \overrightarrow{z_0})$$

$$\cos(\beta_1) = -\overrightarrow{y_0} \cdot \text{proj}_{Q_{xoz}} \overrightarrow{V_{oe}}$$

Hence

$$\beta_1 = \text{atan2}(\det_{\beta_1}, \cos(\beta_1)) \quad (11)$$

#### • Joint angle $\beta_2$

From Fig.6,  $\beta_2$  can be written as follows:

$$\beta_2 = \frac{\pi}{2} - \gamma_2$$

$\gamma_2$  is expressed by the formula bellow:

$$\gamma_2 = \text{atan2}(\det_{\gamma_2}, \cos(\gamma_2)).$$

Where

$\gamma_2$  is the angle between  $\overrightarrow{z_0}$  and  $\overrightarrow{V_{oe}}$



$\vec{z}_0$  and  $\vec{V}_{oe}$  are, respectively, the cosine vector of  $z_0$ -axis of fixed frame at shoulder and the vector between shoulder and elbow points.

$$\cos(\gamma_2) = \vec{z}_0 \cdot \vec{V}_{oe} \text{ and } \det_{\gamma_2} = \det[\vec{n}_{q1} \vec{z}_0 \vec{V}_{oe}]^T$$

So

$$\beta_2 = \frac{\pi}{2} - \text{atan2}(\det_{\gamma_2}, \cos(\gamma_2)) \quad (12)$$

- Joint angle  $\beta_3$

The arguments for the angle  $\beta_3$  are given bellow

$$\cos(\beta_3) = \vec{n}_{q1} \cdot \vec{n}_{q2} \text{ and } \det_{\beta_3} = \det[\vec{V}_{eo} \vec{n}_{q1} \vec{n}_{q2}]^T.$$

So

$$\beta_3 = \text{atan2}(\det_{\beta_3}, \cos(\beta_3)) \quad (13)$$

Where

$\vec{n}_{q1}$  and  $\vec{n}_{q2}$  are respectively, the normal vectors of  $Q_1$ -plan and  $Q_2$ -plan. The first one is defined by two vectors  $\vec{z}_0$  and  $\vec{V}_{oe}$ . The second one is defined by two vectors  $\vec{V}_{oe}$  and  $\vec{V}_{ew}$ .

- Joint angle  $\beta_4$

The joint angle  $\beta_4$  is an angle between  $\vec{V}_{oe}$  (arm) and  $\vec{V}_{ew}$  (forearm) as illustrated in Fig.6. Where  $\vec{n}_{oe}$  and  $\vec{n}_{ew}$  respectively are the normalized vectors of  $\vec{V}_{oe}$  and  $\vec{V}_{ew}$ .

The arguments for the angle  $\beta_4$  are:  $\cos(\beta_4) = \vec{n}_{oe} \cdot \vec{n}_{ew}$  and  $\det_{\beta_4} = \det[\vec{n}_{q1} \vec{n}_{oe} \vec{n}_{ew}]^T$

So

$$\beta_4 = \text{atan2}(\det_{\beta_4}, \cos(\beta_4)) \quad (14)$$

- Joint angle  $\beta_5$

The joint angle  $\beta_5$  is defined between the vectors  $\vec{n}_{q2}$  and  $\vec{A}_6 = (a_x, a_y, a_z)^T$  of the  $z_6$ -axis as illustrated in Fig.6. Thus,  $\beta_5$  is expressed in (15) as follows

$$\beta_5 = \text{atan2}(\det_{\beta_5}, \cos(\beta_5)) \quad (15)$$

Where

$$\cos(\beta_5) = \vec{n}_{q2} \cdot \vec{A}_6 \text{ and } \det_{\beta_5} = \det[\vec{n}_{we} \vec{n}_{q2} \vec{A}_6]^T.$$

- Joint angle  $\beta_6$

The joint angle  $\beta_6$  is the angle between the forearm and the hand of the robot. It is defined by the vectors  $\vec{V}_{ew}$  (elbow-wrist) and  $\vec{V}_{wd}$  (wrist-desired position) (Fig.6). Thus,  $\beta_6$  is the angle between two vectors:  $\vec{n}_{ew} = \frac{1}{|\vec{V}_{ew}|} \vec{V}_{ew}$  and  $\vec{S}_6 = (s_x, s_y, s_z)^T$ .

Consequently, the two arguments of  $\beta_6$  are given below

$$\cos(\beta_6) = \vec{n}_{ew} \cdot \vec{S}_6 \text{ and } \det_{\beta_6} = \det[\vec{A}_6 \vec{n}_{ew} \vec{S}_6]^T.$$

Finally,  $\beta_6$  is expressed by (16)

$$\beta_6 = \text{atan2}(\det_{\beta_6}, \cos(\beta_6)) \quad (16)$$

#### 4) Inverse Kinematic Modeling of the Lower Limb (Leg).

The leg, with 06 degrees of freedom (right or left), is composed of three links that are connected to each other (Fig.7). After calculating the position of the ankle and the knee, we proceed to identify the joint angles of this latter.

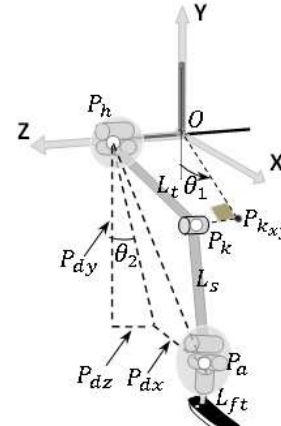


Fig.7: Geometric description of  $\theta_1$  and  $\theta_2$

- Joint angle  $\theta_1$

The joint angle  $\theta_1$  can be calculated via (17) using (3) with the help of the following three vectors:  $\vec{OZ}$ ,  $\vec{OY}$ ,  $\vec{OP}_{kxy}$ .

$$\theta_1 = a \tan 2(\det_{\theta_1}, \cos \theta_1) \quad (17)$$

Where

$$\det_{\theta_1} = \det(\vec{OZ}, \vec{OP}_{kxy}, -\vec{OY})$$

$$\cos \theta_1 = \cos(\vec{OP}_{kxy}, -\vec{OY})$$

$\vec{OZ} = (0,0,1)$ ,  $\vec{OY} = (0,1,0)$  two units vectors of the hip's frame.

$\vec{OP}_{kxy} = (P_{kx}, P_{ky}, 0)$  is the projection of knee's point on  $xy$ -plane that is defined by axes  $\vec{OX}$  and  $\vec{OY}$  of the hip's frame.

- Joint angle  $\theta_2$

From Fig.7, these three points:  $P_h$  (hip's point),  $P_k$  (knee's point), and  $P_a$  (ankle's point) belong to the same plane which is initially parallel to  $XY$ -plane can move laterally only by the joint  $\theta_2$ .

Therefore, the joint angle  $\theta_2$  can be calculated by (18) as follows

$$\theta_2 = \arccos\left(\frac{P_{az}}{P_{ay}}\right) \quad (18)$$

Where

$(P_{ax}, P_{ay}, P_{az})^T$  are the coordinates of the vector  $\vec{V}_{oa}$  that is defined between the origin of hip's frame and the ankle.

- Joint angle  $\theta_3$

From Fig.8, the triangular formula bellow is defined

$$r_{ha}^2 = L_s^2 + L_l^2 - 2 L_s L_l \cos \alpha$$

Where

$$r_{ha} = P_{ax}^2 + P_{ay}^2 + P_{az}^2$$

$L_s$ : length of the shin.

$L_l$ : length of the leg.

From the above equality, the angle  $\alpha$  (between two links: leg and shin) is expressed in (19) bellow

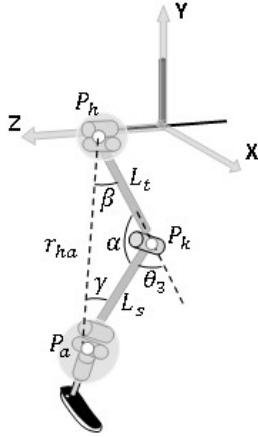


Fig.8: Geometric description of  $\theta_3$ .

$$\alpha = \arccos\left(\frac{r_{ha}^2 - L_{tb}^2 + L_J^2}{2 L_{tb} L_J}\right) \quad (19)$$

Therefore, from Fig.8 and using (19),  $\theta_3$  is obtained through (20).

$$\theta_3 = \pi - \alpha \quad (20)$$

- Joint angle  $\theta_4$  and  $\theta_5$

A new orthonormal frame  $F_A(A, x_A, y_A, z_A)$  is defined at ankle point, where the position of  $L_f$  will be treated as a case of spherical coordinates by  $\theta_4$  and  $\theta_5$  (Fig.9).

Let  $P_Q$  be the plane by the normal vector  $\vec{n}_{ka} = (a, b, c)^T$  expressed in (21)

$$P_Q: a x + b y + c z + D = 0 \quad (21)$$

Where

$$D = a P_{kx} + b P_{ky} + c P_{kz}$$

And the constants  $a, b, c$  are the components of normal vector  $\vec{n}_{ka}$  written in (22)

$$\vec{n}_{ka} = \frac{1}{\sqrt{V_{kax}^2 + V_{kay}^2 + V_{kaz}^2}} (V_{kax}, V_{kay}, V_{kaz}) \quad (22)$$

Given that :  $\vec{n}_{ka}$  : Normal vector of the plane  $P_Q$  deduced from the vector  $\vec{V}_{ka}$  defined by the points of the knee and the ankle.

Using (21) and (22), the axes of the new orthonormal frame  $F_A(A, x_A, y_A, z_A)$  are defined bellow

$\vec{x}_A = (x1_A, x2_A, x3_A) : \vec{n}_{ka} = (a, b, c)^T$ : Normal vector of the plane  $P_Q$

$\vec{z}_A = (z1_A, z2_A, z3_A) : \text{proj}_{P_Q} \vec{z}_0$ : Projection of  $\vec{z}_0$  onto the plane  $P_Q$

$\vec{y}_A = (y1_A, y2_A, y3_A)$ : Cross product of  $\text{proj}_{P_Q} \vec{z}_0$  and  $\vec{n}_{ka}$

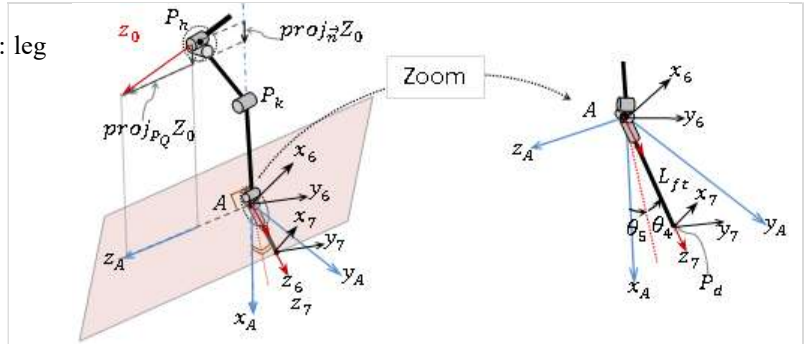


Fig.9: Geometric description of  $\theta_4$  and  $\theta_5$  into the new frame  $R_A(A, x_A, y_A, z_A)$ .

Consequently, the new frame  $F_A(A, x_A, y_A, z_A)$  can be described into the hip's frame by the following matrix.

$$T_{ha} = \begin{bmatrix} x_{A1} & y_{A1} & z_{A1} & P_{Ax} \\ x_{A2} & y_{A2} & z_{A2} & P_{Ay} \\ x_{A3} & y_{A3} & z_{A3} & P_{Az} \\ 0 & 0 & 0 & 1 \end{bmatrix}$$

Thus, one can express the determination of the coordinates of point  $P_d$  in the new frame  $F_A$  as follows

$${}^{R_A}P_d = [T_{ha}]^{-1} {}^{R_0}P_d \quad (23)$$

Finally, from the coordinates  ${}^{R_A}P_d$  given by (23), the determination of the rotational joints  $\theta_4$  and  $\theta_5$  is carried out using the spherical coordinates of the radius  $L_f$ , the foot link, (or  $L_{ad}$ , the length between the ankle and the desired position).

$$\begin{cases} {}^{R_A}P_{dx} = L_f \cos \theta_4 \\ {}^{R_A}P_{dy} = L_f \sin \theta_4 \cos \theta_5 \\ {}^{R_A}P_{dz} = L_f \sin \theta_4 \sin \theta_5 \end{cases} \quad (24)$$

Finally, from (24),  $\theta_4$  and  $\theta_5$  can be expressed by (25) and (26) bellow

$$\theta_4 = \arccos\left(\frac{{}^{R_A}P_{dx}}{L_P}\right) \quad (25)$$

And

$$\theta_5 = \arctan\left(\frac{{}^{R_A}P_{dz}}{{}^{R_A}P_{dy}}\right) \quad (26)$$

- Joint angle  $\theta_6$

The last rotational joint  $\theta_6$  (See Fig.10) of the leg can be obtained through a simple matrix calculation given by (27).

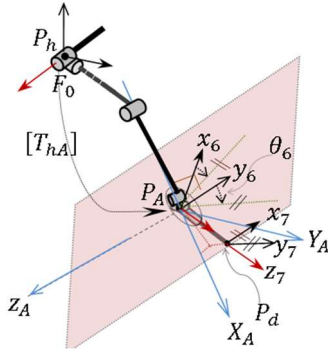


Fig.10: Geometric definition of  $\theta_6$  of the leg.

$$\begin{aligned} {}^0T_7 &= {}^0T_4 {}^4T_5 {}^5T_6 {}^6T_7 \\ \Rightarrow {}^6T_7 &= [{}^5T_6]^{-1} [{}^4T_5]^{-1} [{}^0T_4]^{-1} [{}^0T_7] \end{aligned} \quad (27)$$

Where

${}^0T_7$ : Matrix of the given situation of the end effector (foot position).

${}^0T_4$ : Matrix of the situation of the frame  $R_A$  inserted at the robot's ankle. This matrix is none other than the matrix  $T_{ha}$

$$[{}^0T_4] = [T_{ha}] = [{}^0T_1] [{}^1T_2] [{}^2T_3] [{}^3T_4]$$

${}^6T_7$ : Transformation matrix between  $R_6$  and  $R_7$  which is expressed by  $\theta_6$ .

The components of the matrix  ${}^6T_7$  are given below:

$${}^6T_7 = \begin{bmatrix} \cos \theta_6 & -\sin \theta_6 & 0 & 0 \\ \sin \theta_6 & \cos \theta_6 & 0 & 0 \\ 0 & 0 & 1 & L_p \\ 0 & 0 & 0 & 1 \end{bmatrix}$$

Thus, (27) can be reformulated as follows:

$${}^6T_7 = [{}^5T_6]^{-1} [{}^4T_5]^{-1} [T_{ha}]^{-1} [{}^0T_7] \quad (28)$$

By identifying the terms in (28),  $\theta_6$  can be easily found in (29).

$$\theta_6 = a \tan 2(\sin \theta_6, \cos \theta_6) \quad (29)$$

**Note.**

Due to symmetry of robot, the same modeling procedure used for the right leg will be applied to the left leg.

#### IV. PARAMETRICS EQUATIONS OF END-EFFECTOR'S TRAJECTORIES

In order to verify the obtained results of the used approach in solving IK problem of biped robot, we plan to conduct simulations using Matlab software and leveraging the solutions the previously obtained results. However, it is necessary to determine the set of trajectories for the various members of the robot.

##### A. The trajectory of the hip.

The trajectory of the hip is defined by the three parametric equations below: (30), (31) and (32)

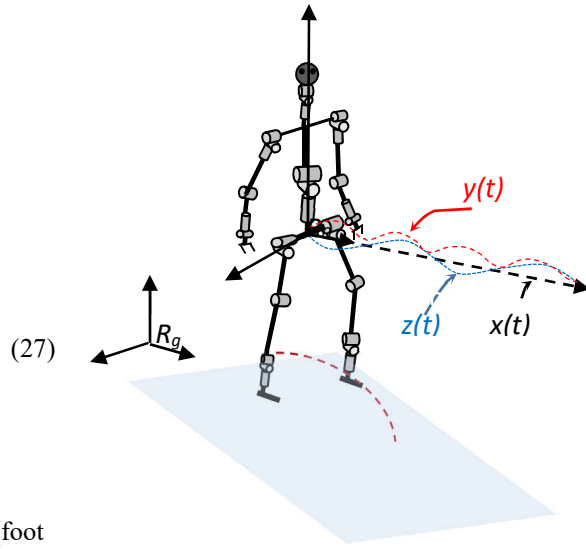


Fig.11: Trajectory hodograph of the hip.

$x_h(t)$ : Linear equation on x-axis.

$$x_h(t) = at + b \quad (30)$$

$y_h(t)$ : Polynomial equation of degree five in the plane (o:x,y).

$$y_{hs}(t) = k_0 + k_1t + k_2t^2 + k_3t^3 + k_4t^4 + k_5t^5 \quad (31)$$

$z_h(t)$ : Sinusoidal equation in the plane (o: x, z)

$$z(t) = A_z \sin(a(x(t) - x_0)) \quad (32)$$

##### B. Trajectory of the foot in flight.

Let  $X_{ps}(t)$  and  $X_{pd}(t)$  denote the functions expressing respectively the trajectories of the simple support Phase (SSP) and the double support phase (DSP). Given that.

$$\begin{aligned} X_{ps}(t) &: \{x_{ps}(t), y_{ps}(t), z_{ps}(t)\} & \text{and} \\ X_{pd}(t) &: \{x_{pd}(t), y_{pd}(t), z_{pd}(t)\} \end{aligned}$$

Where

$\{x_{ps}(t), y_{ps}(t), z_{ps}(t)\}$  and  $\{x_{pd}(t), y_{pd}(t), z_{pd}(t)\}$  denote its parametric equations expressed in the principal frame. However, the double support phase represents 20% of the single support phase [9].

$x_h(t)$ : Cubic polynomial equation.

$$x_{ps}(t) = a_0 + a_1t + a_2t^2 + a_3t^3 \quad (33)$$

$y_h(t)$ : Quintic polynomial equation.

$$y_{ps}(t) = b_0 + b_1t + b_2t^2 + b_3t^3 + b_4t^4 + b_5t^5 \quad (34)$$

$z_h(t)$  : no movement of the foot along the z-axis.

$$z_p(t) = 0 \quad (35)$$

### C. Trajectory of the upper limbs.

The two upper limbs swing in an alternating and opposite manner between a forward and backward movement. (Fig. 12).

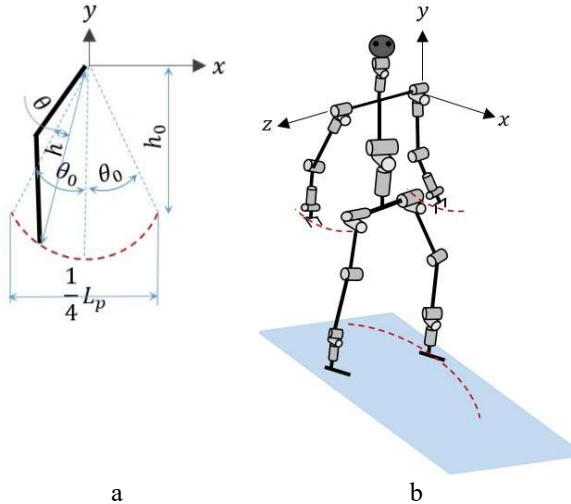


Fig.12: Hodograph of the robot's upper limbs.

Their parametric equations with respect to the shoulder frame are expressed by the following equations

$x_m(t)$  : Linear equation along the x-axis.

$$x_m(t) = at + b \quad (36)$$

$y_m(t)$  : Cosinusoidal equation

$$y_m(t) = -R \cos \theta(t) \quad (37)$$

Where:

$$R \leq L_a + L_{fa}$$

$$\theta(t) = \frac{2}{T_c} \theta_0 t - \theta_0 : \text{Linear equation.}$$

$z_h(t)$  : No movement of the foot along the z-axis.

$$z_m(t) = 0 \quad (38)$$

**Note.**

All the constants in the parametrics equations (30-38) of trajectories are detrmned with respect to condition and exigences of walk of robot. Primarily, bellow parameters are used:

$L_p$  : Step length.

$T_s$  : Step period for the SSP.

$T_d$  : Step period for the DSP.

$H_f$  : Maximum height of the flight foot.

$S_f$  : Corresponding abscissa to  $H_f$ .

$H_{max}$  and  $H_{min}$  : Respectively, maximum and minimum height of the hip .

$H_{x_0}$  : Hip initial position on x-axis.

## V. SIMULATION OF INVERSE KINEMATIC MODEL OF THE BIPED ROBOT

The simulations are conducted on the bipedal robot to validate the IKM solutions obtained previously. The bipedal robot should walk correctly by following the trajectories imposed on its gait-members (hip, upper limbs, and lower limbs).

### Simulation parameters values.

- Lengths of links of robot are given in Tab.1.
- Maximum and minimum height of the hip respectively :  $h_{max} = 0.69$ ;  $h_{min} = 0.66[m]$
- Maximum foot height in flight:  $H_f = 0.10[m]$ .
- One-step period :  $T_p = T_s + T_d = 1.3 + 0.3 = 1.6[s]$
- Average time corresponding to  $H_f$ :  $T_m = T_s / 2[s]$
- Step length:  $L_p = 0.32[m]$ .
- Final position of the hip in DSP :  $H_{x_f} = 0.5.L_p + H_{x_0} \cdot [m]$

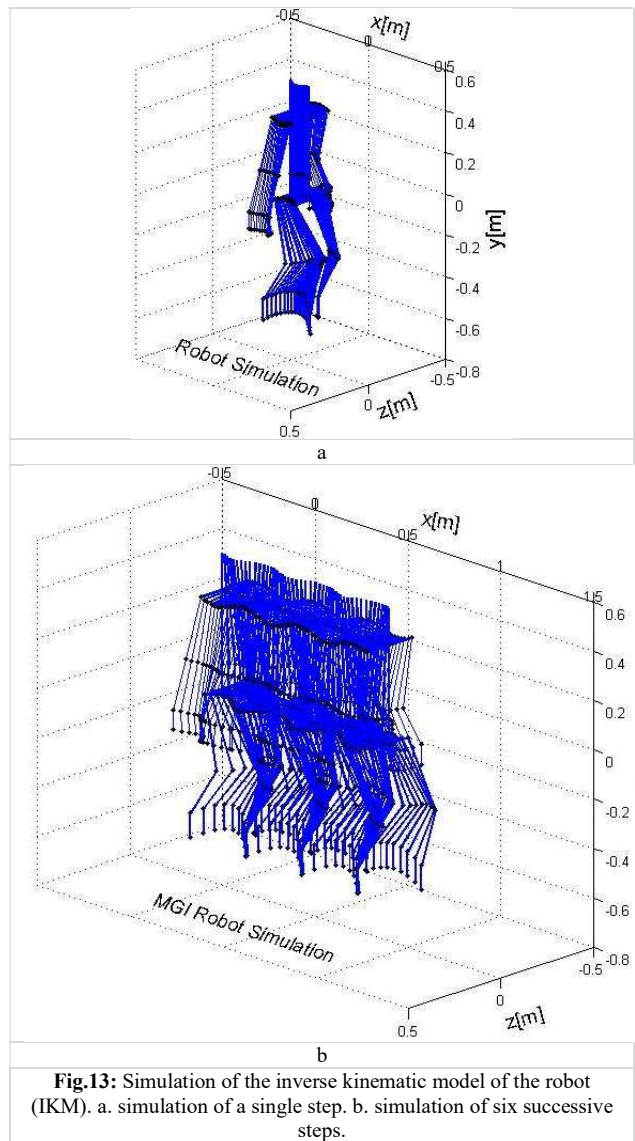


Fig.13: Simulation of the inverse kinematic model of the robot (IKM). a. simulation of a single step. b. simulation of six successive steps.

These simulations, depicted in Fig.13, demonstrates that the developed solutions in solving IKM presented above is correct and accurate.

## VI. GENERAL CONCLUSION

An attractive and basic topic in robotics was developed in this work. An application on biped robot with 30 degree of freedom was presented. Topologically, this robot consists of a central mechanism (the trunk), two upper limbs (right arm and left



arm), two lower limbs (right leg and left leg), and a neck-head mechanism.

This work extends to inverse kinematic modeling by employing an alternative approach based on vectors and the geometric environment of the robot. This approach offers a significant advantage in obtaining solutions through linear and uncoupled equations. In fact, all joint variables of the bipedal robot with 30 degrees of freedom are determined using this approach. Simulations were conducted and the obtained results align with the expected goals. Thus, this work contributes to the advancement of knowledge in the field of robotics.

#### REFERENCES

- [1] A. Singh, A. Singla. Kinematic Modeling of Robotic Manipulators. Proc. Natl. Acad. Sci., India, Sect. A Phys. Sci. pp.303–319, 2017. DOI: 10.1007/s40010-016-0285-x
- [2] M.Menad, z. Derouiche, Z-A. Foitih, W. Nouibat. Kinematic modeling of a humanoid robot with 18 DOF in a virtual environment. IEEE 3rd Inter. Conf. on Innov. Comp. Tech. (INTECH 2013),2013. DOI: 10.1109/INTECH.2013.6653656
- [3] W-A. Bin Wan Daud, W. Faizura, M. Azmi Adly, I. Elamvazuthi, M. Begam. Kinematic modeling of humanoid arm. IEEE Inter. Conf. on Intell. and Adv. Syst.. 2011. DOI: 10.1109/ICIAS.2010.5716210
- [4] W. Dewandhana, K. I. Apriandy, B. S. B. Dewantara, D. Pramadihanto. Forward Kinematics with Full-Arm Analysis on “T-FLoW” 3.0 Humanoid Robot. International Electronics Symposium. IES) 2021.
- [5] Y.Liu, J. Weng, F. Wang, J. Tang et all. Design and Control of the Biped Robot HTY. Springer nature Singapore. ICIRA 2023, LNAI 14270, pp. 404–415, 2023.
- [6] J. Lee and H-M. Joe. Design of Humanoid Robot Foot to Absorb Ground Reaction Force by Mimicking Longitudinal Arch and Transverse Arch of Human Foot. 2023. Springer International Journal of Control, Automation, and Systems 21(11) (2023) 3519-3527
- [7] N. Hadidi, M. Bouaziz, C. Mahfoudi, M. Zaharuddin. Geometric Approach to Solve Inverse Kinematics of Six DoF Robot With Spherical Joint. Acta polytechnica, 63(5), pp. 326–346. <https://doi.org/10.14311/ap.2023.63.0326>
- [8] T. Lyche. A short review of linear algebra. Numerical Linear Algebra and Matrix Factorizations. Springer Nature, Switzerland AG:15-18, 2020. <https://doi.org/10.1007/978-3-030-36468-7-1>.
- [9] Z. Tang, C. Zhou & Z. Sun. Trajectory Planning for Smooth Transition of a Biped Robot. IEEE Intern. Conf. of Robotics & Automation. Taiwan.. vol.2. Issue: 14-19 . pp. 2455- 2460. 2003

**Nacer Hadidi** was born in Bouira, Algeria, in 1980. He received the Engineer's degrees in Mechanical Engineering from University of Blida Saad Dahleb in 2004, the Magister degree from Ecole Nationale Polytechnique, Algiers, in 2010. He is currently a Ph.D student at the Mechanical Department at the same establishment. His interest research area is mechanisms and robotics. He is an assistant professor at Ecole Nationale Supérieure des Technologies avancées since 2012 in Algiers.

**Chawki Mahfoudi** is a Professor at Department of mechanical engineering of university of Larbi ben M'hidi in Oum El Bouaghi, Algeria. He held different positions in this University. He was the head of mechanical engineering department. Currently, He is the Dean of the same university. His interest research is robotics and control.

**Mohamed Bouaziz** was a Professor at Departement of Mechanical engineering at Ecole Nationale Polytechnique, Algeria. He spend more than 30 years at Ecole Nationale Polytechnique, teaching and supervising.

**Zaharuddin Mohamed** is a Professor at Universiti Teknologi Malaysia (UTM), School of Electrical Engineering. He graduated and obtained bachelor degree in Electrical, Electronics and Systems Engineering at Universiti Kebangsaan Malaysia, Malaysia, in 1993. In 1995, He got Master of Science in Control Systems Engineering from the University of Sheffield, UK. He conducted his PhD at the same university in Control Engineering in UK, in 2003. His interest area of research is control of under-actuated systems, robotics, and mechatronics.

**Ahcene Bouzida** was born in Medea, Algeria, in 1981. He performed his study at Department of Electrical Engineering at Ecole Nationale Polytechnique of Algiers, Algeria, where He graduated and obtained his Engineer, Master and PhD diploma respectively in 2004, 2007 and 2011. Now, He is a Professor at University of Bouira-M'hand Oulhadj, department of electrical engineering.